AMERICAN SOCIETY FOR MICROBIOLOGY | Antimicrobial Agents and Chemotherapy

Hepatitis C Virus RNA-Dependent RNA Polymerase Interacts with the Akt/PKB Kinase and Induces Its Subcellular Relocalization

María Llanos Valero,[a]* Rosario Sabariegos,[a,d] Francisco J. Cimas,[b] Celia Perales,[e,f,i] Esteban Domingo,[e,f,g] Ricardo Sánchez-Prieto,[b,g,h] Antonio Mas[a,c,g]

Laboratorio de Virología Molecular[a] and Laboratorio de Oncología Molecular,[b] Centro Regional de Investigaciones Biomédicas (CRIB), Universidad de Castilla-La Mancha, Albacete, Spain; Facultad de Farmacia[c] and Facultad de Medicina,[d] Universidad de Castilla-La Mancha, Albacete, Spain; Centro de Biología Molecular "Severo Ochoa," CSIC-UAM, Cantoblanco, Madrid, Spain[e]; Centro de Investigación Biomédica en Red de Enfermedades Hepáticas y Digestivas (CIBERehd), Barcelona, Spain[f]; Unidad de Biomedicina UCLM-CSIC[g] and Parque Científico y Tecnológico de Albacete (PCyTA),[h] Albacete, Spain; Liver Unit, Internal Medicine, Laboratory of Malalties Hepàtiques, Vall d'Hebron Institut de Recerca-Hospital Universitari Vall d'Hebron, (VHIR-HUVH), Universitat Autònoma de Barcelona, Barcelona, Spain[i]

Hepatitis C virus (HCV) interacts with cellular components and modulates their activities for its own benefit. These interactions have been postulated as a target for antiviral treatment, and some candidate molecules are currently in clinical trials. The multifunctional cellular kinase Akt/protein kinase B (PKB) must be activated to increase the efficacy of HCV entry but is rapidly inactivated as the viral replication cycle progresses. Viral components have been postulated to be responsible for Akt/PKB inactivation, but the underlying mechanism remained elusive. In this study, we show that HCV polymerase NS5B interacts with Akt/PKB. In the presence of transiently expressed NS5B or in replicon- or virus-infected cells, NS5B changes the cellular localization of Akt/PKB from the cytoplasm to the perinuclear region. Sequestration of Akt/PKB by NS5B could explain its exclusion from its participation in early Akt/PKB inactivation. The NS5B-Akt/PKB interaction represents a new regulatory step in the HCV infection cycle, opening possibilities for new therapeutic options.

Hepatitis C virus (HCV) is a positive-strand RNA virus [RNA(+)] responsible for chronic infections in almost 200 million people worldwide. HCV-positive patients are at high risk of developing cirrhosis and hepatocellular carcinoma (1). As an obligate parasite, HCV usurps cellular functions and pathways to complete its replication cycle, and some of these routes are related to cell cycle control (2). The Akt/protein kinase B (PKB) family of serine/threonine protein kinases are involved in several signaling pathways that can impact the outcome of viral infections. Akt/PKB resides in the cytosol in an inactive conformation. Initial stimulation of the cell causes activation of a cell surface receptor and subsequently phosphorylation of phosphatidylinositol 3-kinase (PI3K). Activated PI3K is responsible of the formation of phosphatidylinositol(3,4,5)-trisphosphate second messenger. Akt interacts with these phosphoinositides and is recruited to the membrane, where it can be fully activated by PDK1 and other kinases. The Akt/PKB pathway is involved in processes as disparate as nutrient metabolism, regulation of protein synthesis, autophagy, and the balance of apoptosis versus cell survival and proliferation, the latter being critical for the outcome of viral infections (3–6). Akt/PKB can influence the virus-host interaction by several mechanisms. The translational repressors 4E-BPs are eukaryotic translation initiation factor 4E (eIF4E)-binding proteins that prevent cap-dependent translation of cellular mRNAs. Akt/PKB is needed for the inactivation of 4E-BPs, which occurs through a phosphorylation reaction that requires FRAP/mammalian target of rapamycin (mTOR) and results in activation of cellular translation (7). Akt/PKB is the downstream target of the lipid kinase PI3K, and both are involved in cell proliferation and apoptosis. In infections of neuronal cells by dengue virus serotype 2 (dengue-2) and Japanese encephalitis virus, PI3K played an antiapoptotic role, and the blocking of PI3K activation enhanced virus-induced cytopathology with no effect on virus production (8). These multiple effects of Akt/PKB can modulate cap- versus internal ribosome entry site (IRES)-dependent translation as well as infected-cell survival, which may facilitate virus persistence. Thus, not surprisingly, several viral proteins can modulate PI3K/Akt-dependent signaling pathways (9–12).

We are interested in the viral and cellular factors that may modify the replicative fitness of HCV, thereby permitting HCV persistence, a hallmark of the infection by this virus *in vivo*. No unified picture has been derived from previous descriptions of the interaction of HCV and Akt/PKB-dependent pathways. An early and transient activation of the PI3K/Akt/mTOR pathway by the HCV E2 glycoprotein resulted in enhancement of HCV entry into the cell (13). This activation took place 15 min postinfection (p.i.), but at 24 h p.i. the levels of activated Akt/PKB were no longer significant. Since inactivation of PI3K/Akt required infectious virus, the involvement of HCV gene prod-

Received 21 December 2015 **Returned for modification** 1 February 2016
Accepted 18 March 2016

Accepted manuscript posted online 28 March 2016

Citation Valero ML, Sabariegos R, Cimas FJ, Perales C, Domingo E, Sánchez-Prieto R, Mas A. 2016. Hepatitis C virus RNA-dependent RNA polymerase interacts with the Akt/PKB kinase and induces its subcellular relocalization. Antimicrob Agents Chemother 60:3540–3550. doi:10.1128/AAC.03019-15.

Address correspondence to Antonio Mas, Antonio.Mas@uclm.es.

* Present address: María Llanos Valero, Instituto de Investigación en Discapacidades Neurológicas (IDINE), Universidad de Castilla–La Mancha, Albacete, Spain.

M.L.V., R.S., and F.J.C. contributed equally to this work.

Supplemental material for this article may be found at http://dx.doi.org/10.1128/AAC.03019-15.

ucts in the inactivation was postulated (13). Chemical Akt/PKB inhibition with Akt-II and Akt-V inhibitors as well as genetic inhibition with small interfering RNAs (siRNAs) resulted in a reduction of infectivity (13). Furthermore, such inactivation and the downstream inhibition of the PI3/Akt/mTOR pathway resulted in HCV-induced autophagy (14), which may contribute to membrane rearrangements to accommodate replication complexes (15, 16). Similar results have been recently observed using mTOR inhibitors (17). How the transition of Akt/PKB from an early-activated plasma membrane-bound form to a cytoplasm location takes place is not known.

In the present report, we describe a new functional activity of the HCV polymerase NS5B that consists of interaction with Akt/PKB, resulting in translocation of this key kinase from the cytoplasm to the perinuclear region, where the two proteins colocalize. This Akt/PKB relocalization may be an additional mechanism of temporal modulation of its cytoplasmic activity and recruitment to assist in replicative functions. Akt/PKB relocalization by virtue of its interaction with NS5B could have additional consequences for HCV, from limitation of cell entry to phosphorylation of viral components of the replicative complexes. Several Akt/PKB inhibitors are currently in clinical trials, and this signaling pathway could be also targeted for treatment of HCV infection.

MATERIALS AND METHODS

Reagents, expression plasmids, and inhibitors. Plasmid pDest14-NS5BΔ21-FP encoding HCV NS5B fused to citrine and plasmid pRSET-citrine, which encodes citrine, as well as vectors to overexpress Akt/PKB tagged with the hemagglutinin (HA) epitope (pcFEL) and NS5B tagged with citrine (pcDNA-Dest40-NS5B-citrine), have been described previously (18, 19). Recombinant Akt/PKB was purchased from Biaffin (Biaffin GmbH & Co), Akt/PKB inhibitor MK2206 from Selleckchem, Lipofectamine 2000 from Invitrogen, and G418 from Lonza. Huh7.5 cells and HCV subgenomic replicon pI389/NS3-3′/LucUbiNeo-ET were kindly provided by R. Bartenschlager (University of Heidelberg, Heidelberg, Germany) (20). The following antibodies were used: anti-HA (BAbCo), anti-green fluorescent protein (anti-GFP; Covance), anti-NS5B (ab35586; Abcam), anti-Akt and anti-pAkt$_{s473}$ (Cell Signaling Technology), and anti-tubulin (Santa Cruz Technology). Alexa Fluor 488- and 546-conjugated antibodies (Invitrogen) were used as fluorescent secondary antibodies.

HCV NS5BΔ21-FP and GFP purification. Point mutants in NS5BΔ21 fused to citrine were generated by site-directed mutagenesis according to the manufacturer's instructions (QuikChange site-directed mutagenesis; Agilent Technologies). Synthetic oligonucleotides used for point mutant generation are described in Table S1 in the supplemental material, and chromatograms from sequencing results are shown in Fig. S1B in the supplemental material. Wild-type NS5BΔ21 and mutants of NS5BΔ21 fused to citrine as well as recombinant citrine were overexpressed and purified as described previously (19, 21). Briefly, *Escherichia coli* Rosetta cells (Novagen) were transformed with construct pDest14-NS5BΔ21-FP, encoding the NS5B-FP fusion protein, or with pRSET-citrine, encoding recombinant citrine protein. Cells expressing the protein of interest were collected, and the protein was purified by affinity chromatography. SDS-PAGE and Coomassie blue staining were performed to evaluate the purification steps. Fractions showing the purest and most concentrated protein were pooled, dialyzed against dialysis buffer (20 mM Tris-HCl [pH 7.0], 1 M NaCl, 10% glycerol), and stored at 4°C. SDS-PAGE and Coomassie blue staining were used to monitor all purification steps. Final purified proteins were quantified by densitometry. Only proteins with at least 95% purity as judged by SDS-PAGE and Coomassie blue staining were used for further experiments.

***In vitro* kinase assay.** HCV NS5B-FP, NS5B-FP point mutants, or citrine protein (1.6 μg) was incubated in hot kinase buffer (20 mM HEPES [pH 7.4], 10 mM $MgCl_2$, 10 mM $MnCl_2$, 1 μCi of [γ-^{32}P]ATP, 1 mM dithiothreitol [DTT]) in the presence of 0.5 μg of recombinant Akt/PKB (Biaffin GmbH & Co). The products were separated on an SDS-PAGE gel. After electrophoresis, the gel was dried and radiolabeled products were detected by autoradiography. Alternatively, dried gels were exposed to phosphorimager screens and scanned with Typhoon9600 (Molecular Dynamics).

***In vitro* RNA-dependent RNA polymerase (RdRP) replication assays.** RNA polymerase assays were performed using the symmetric substrate LE-19 (sequence 5′ UGUUAUAAUAAUUGUAUAC 3′), which is capable of *de novo* initiation (DN), primer extension (PE), and template switching (TS) as previously described (19). Except when indicated otherwise, 200 nM NS5B was preincubated for 30 min in a reaction mixture containing 20 mM MOPS (morpholinepropanesulfonic acid) (pH 7.3) and 5 mM $MnCl_2$, in the presence or absence of Akt (0.5 μg of recombinant Akt/PKB [Biaffin GmbH & Co]), and supplemented or not with ATP (500 μM), as indicated in the figure legend. Reactions were started by adding 500 μM GTP, 100 μM ATP and UTP, and 1 μCi [α-^{32}P]CTP (3,000 Ci/mmol; PerkinElmer Life Sciences). Reactions were stopped with EDTA/formamide loading buffer at different time points as indicated. Products were separated using denaturing polyacrylamide (23% phosphonoacetic acid [PAA], 7 M urea) gel electrophoresis. Gels were exposed to phosphorimager screens and scanned with Typhoon (Molecular Dynamics). Quantification was obtained by running samples on parallel gels and determining band volumes using ImageQuant software (GE Healthcare).

***In vitro* transcription, electroporation, and colony formation.** After digestion with ScaI, replicon DNA was extracted with phenol-chloroform. *In vitro* transcription was performed with 1 μg of digested DNA and the Megascript T7 kit (Ambion) according to the manufacturer's instructions. The RNA obtained was purified with the MegaClear kit (Ambion), quantified, and stored at −80°C until use. Huh7.5 cells were electroporated with transcribed RNA from the replicon using the Electrobuffer kit (Cell projects, Iberlabo, Madrid, Spain), in accordance with the manufacturer's instructions. Briefly, exponentially growing cells were harvested and washed with electroporation medium. Four micrograms of replicon RNA and 6 μg of carrier Huh7.5 RNA were mixed with the electroporation medium and added to 4×10^6 cells. The cell suspension was pulsed once with Gene Pulser II (settings, 975 μF and 270 V; Bio-Rad). After electroporation, 2×10^6 cells (and 1/10 and 1/20 dilutions) were seeded on petri dishes in Dulbecco's modified Eagle's medium (DMEM; Sigma-Aldrich Química, Madrid, Spain) with 10% fetal bovine serum (HyClone, Fisher Scientific, Madrid, Spain), supplemented with 1 M HEPES (Sigma), 1% glutamine, nonessential amino acids, antibiotics (penicillin, streptomycin), and sodium pyruvate. Cells were kept at 5% CO_2 and 37°C. Twenty-four hours later, the DMEM culture medium was replaced with fresh medium containing G418 (Labclinics, Barcelona, Spain), after which the medium was refreshed twice per week for 2 weeks.

Cell culture virus infection. The origin of the Huh-7.5 cell line, procedures for cell growth in DMEM, the virus used in the experiments rescued from plasmid Jc1FLAG2(p7-nsGluc2A) (a chimera of J6 and JFH-1 from genotype 2a), and the procedures used to prepare the initial virus stock HCVp0, to titrate viral infectious particles, and to quantify viral RNA have been previously described (23, 24). To perform infections for immunofluorescence and RNA quantification assays, 1×10^5 Huh7.5 cells were infected with HCVp0 at a multiplicity of infection (MOI) of 0.5 50% tissue culture infective dose ($TCID_{50}$)/cell. After 5 h of virus adsorption, supernatants were replaced with fresh medium with or without the inhibitor MK-2206. The infected cells were further incubated at 37°C for 2 h and 43 h. To perform infections with HCVp0 for coimmunoprecipitation assays, 4×10^6 Huh7.5 cells were infected with HCVp0 at an MOI of 0.5 $TCID_{50}$/cell. After 5 h of virus adsorption, supernatants were replaced with 10 ml of fresh medium. The infected cells were further incu-

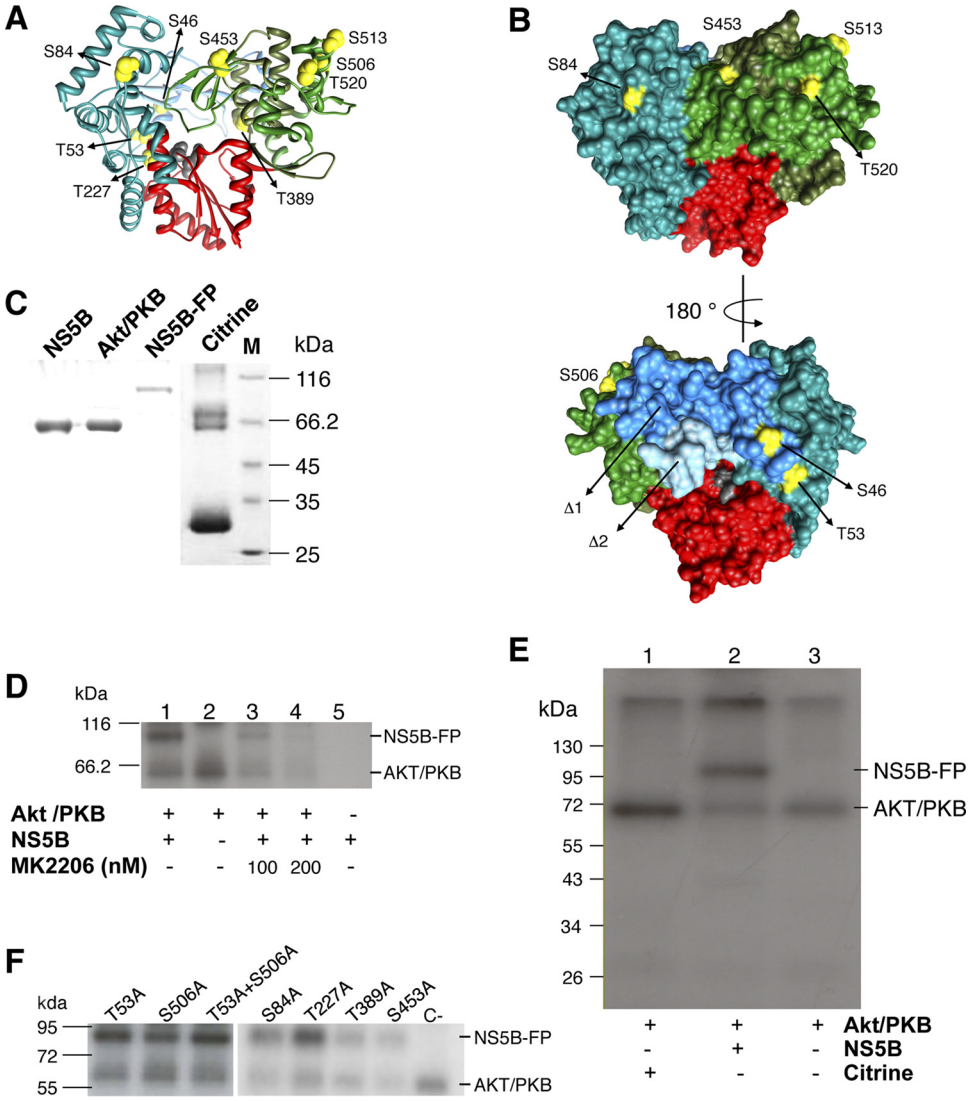

FIG 1 (A) Structure of NS5B. HCV replicase NS5B from strain HC-J4 genotype 1b (47) is depicted in ribbons showing the fingers (blue), palm (red), and thumb (green) domains. Sites that can potentially be phosphorylated by Akt/PKB are depicted as yellow spheres. (B) HCV NS5B surface showing the Akt/PKB phosphorylation sites (yellow) as well as loops Δ1 and Δ2. Color codes are as described for panel A. Ser453, Thr53, Thr520, Ser84, Ser506, Ser46, and Ser513 displayed percentages of relative surface accessibility of 14.5%, 21.7%, 24.5%, 36.2%, 39.7%, 43.5%, and 78.9%, respectively. (C) SDS-PAGE (10%) analysis of proteins NS5B, Akt/PKB, NS5B-FP, and citrine. Molar mass markers are depicted on the right. (D) *In vitro* kinase assay. Reaction products were resolved in a 10% SDS-PAGE gel. Concentration of inhibitor MK-2206 is in nanomolar values. MW, molecular weight (in thousands). (E) *In vitro* kinase assay products resolved in a 12% SDS-PAGE gel, with the assay performed as described for panel D but using recombinant citrine as the substrate for Akt/PKB. In panels D and E, the presence or absence of the different components of the reactions is shown below the gel. (F) *In vitro* kinase assay (as described for panel D) using the indicated NS5B-FP point mutants as the substrate. Positions of protein markers are indicated on the left (panels D to F).

bated at 37°C for 72 h. The absence of contamination was checked by maintaining and titrating mock-infected cells and their supernatants in parallel with the infected cultures. No infectivity in the mock-infected cultures was detected in any of the experiments.

Coimmunoprecipitation. Huh7.5 cells from either transfection or infection experiments were collected 48 h posttransfection or postinfection in HNTG lysis buffer (25 mM HEPES [pH 7.5], 0.3 M NaCl, 1.5 mM $MgCl_2$, 0.2 mM EDTA, 1% Triton X-100, 0.1% SDS, 0.5% deoxycholic acid, 20 mM B-glycerophosphate) containing protease and phosphatase inhibitors (2 μg/ml leupeptin, 2 μg/ml aprotinin, 1 mM phenylmethylsulfonyl fluoride [PMSF], and 0.1 mM Na_3VO_4). Cell lysates were centrifuged at 12,000 × *g* for 1 min at 4°C. Supernatants were recovered, mixed with 1 μg of primary antibody, and incubated for 2 h at 4°C. After this, reaction mixtures were incubated for 3 h with protein G (Gamma Bind Sepharose; Amersham) and washed once in HNTG lysis buffer. Protein G agarose-bound immune complexes were collected by centrifugation at 12,000 × *g* for 1 min and washed once with lysis buffer, and proteins were detected by Western blotting.

Western blot analysis. Protein quantification was performed using the bicinchoninic (BCA) protein assay kit (Pierce, Madrid, Spain) according to the manufacturer's instructions. Samples were separated on 10% SDS-PAGE gels and transferred onto Immobilon-P membranes (Millipore). Membranes were probed with primary antibodies as indicated in the corresponding figures. The proteins were visualized using suitable horseradish peroxidase (HRP)-conjugated secondary antibodies (Santa Cruz Biotechnology). Antibody detection was achieved by enhanced chemiluminescence (Amersham, GE Health Care) in an LAS-3000 system (FujiFilm, Japan). Tubulin was used as a loading control.

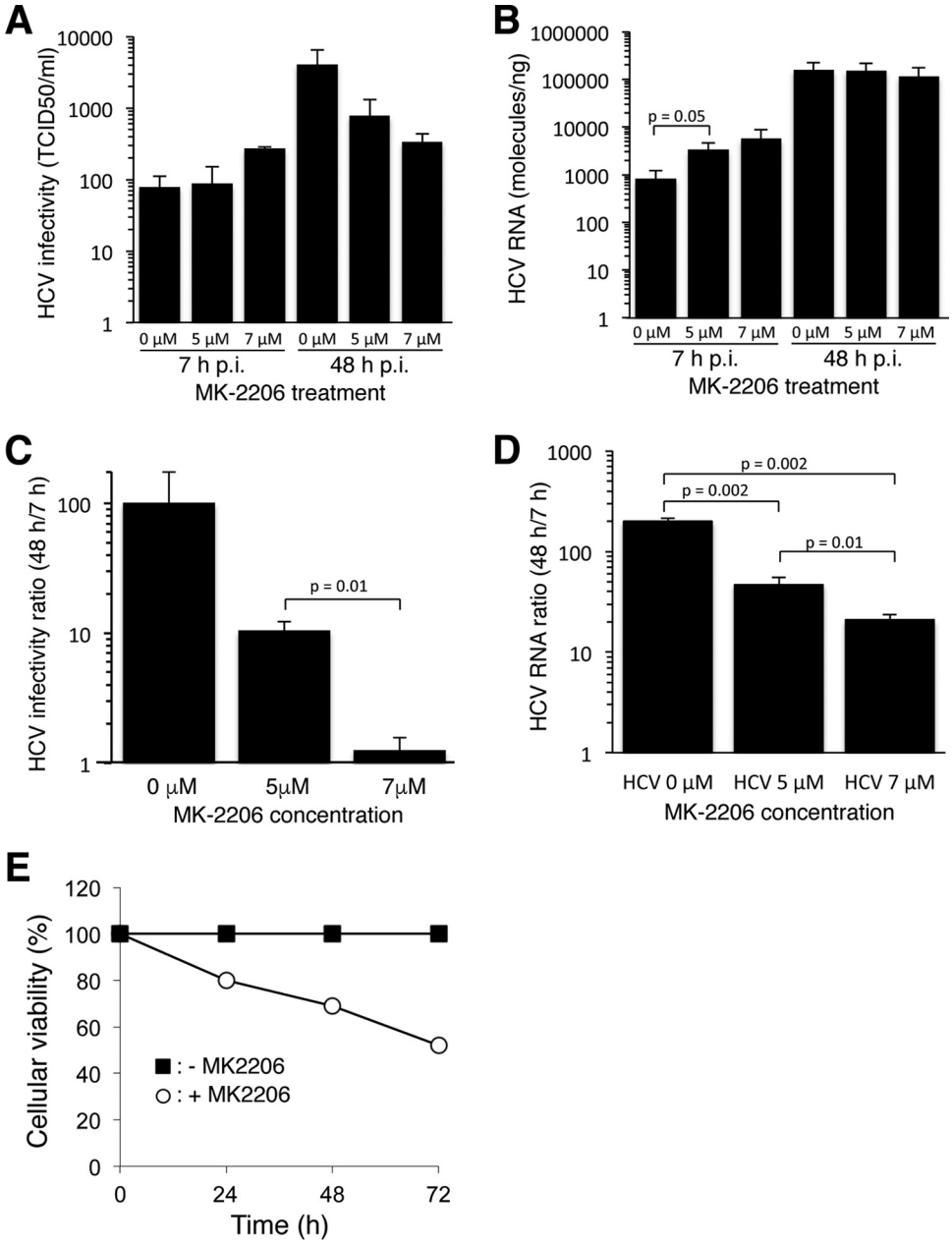

FIG 2 Effects of Akt/PKB inhibition by MK-2206 on HCVp0 replication. (A) Viral titer in the supernatant of infected cultures was sampled at 7 h or 48 h postinfection (p.i.) in the presence of the indicated MK-2206 concentrations. (B) Intracellular HCV RNA at 7 h or 48 h p.i. in the presence of indicated MK-2206 concentrations. (C) Fold changes of viral titer in the supernatant from 7 h to 48 h p.i. (D) Fold changes of intracellular HCV RNA titer from 7 h to 48 h p.i. (E) Viability of Lunet cells in the presence (open circles) or absence (filled squares) of MK-2206 (10 μM). Time zero represents the time at which MK-2206 was added. Values are the averages from three determinations. Standard deviation values are smaller than the graph symbols and therefore not visible. *P* values obtained with Student's *t* tests are shown.

Real-time RT-PCR for RNA quantification. Akt/PKB mRNA was quantified by quantitative real-time PCR (qRT-PCR) using an ABIPrism 7500 FAST Sequence detection system (Applied Biosystems). cDNA was amplified using the SYBR1 Green PCR master mix (Applied Biosystems) in the presence of specific oligonucleotides Akt_sense (5′-ACATCTGTC CTGGCACAC-3′; sense orientation) and Akt_antisense (5′-GCCAGTG CTTGTTGCTTG-3′; antisense orientation). The conditions for RT-PCR amplification and RNA quantification were as previously described (25). Primers for qPCR were designed using Primer Express software, which was provided with the 7000 Sequence detection system (Applied Biosystems). Oligonucleotides were purchased from Thermo Scientific (Madrid, Spain). HCV RNA real-time quantitative RT-PCR was carried out using the Light Cycler RNA Master SYBR green I kit (Roche) according to the manufacturer's instructions. The 5′-untranslated (5′-UTR) noncoding region of the HCV genome was amplified using oligonucleotides HCV-5UTR-F2 (5′-TGAGGAACTACTGTCTTCACGCAGAAAG; sense orientation), and HCV-5UTR-R2 (5′-TGCTCATGGTGCACGGTCTAC GAG; antisense orientation). Quantification was performed relative to a standard curve obtained with known amounts of HCV RNA, synthesized by *in vitro* transcription of plasmid GNN DNA.

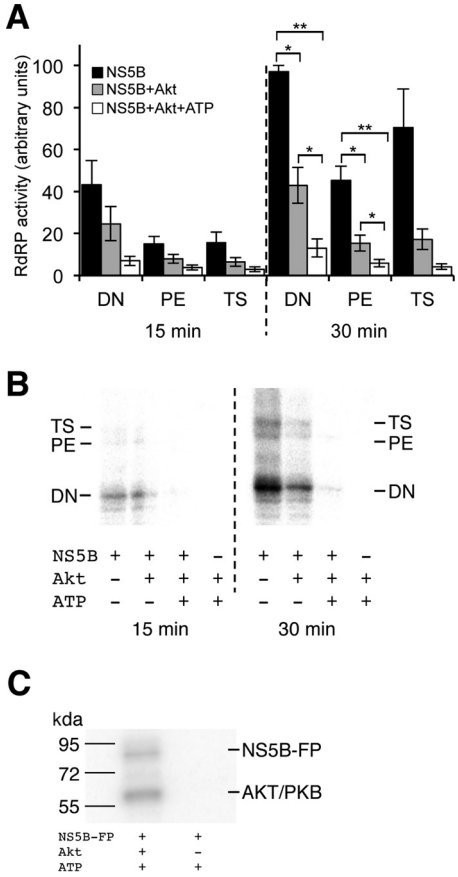

FIG 3 RNA synthesis in the presence of active Akt. (A) RNA-dependent RNA polymerase activity (in arbitrary units) using LE19 RNA as a template under different conditions. HCV NS5B was incubated in MOPS (20 mM) buffer and $MnCl_2$ (5 mM) (black), supplemented with Akt (gray) or Akt plus ATP (white) for 30 min at room temperature. After incubation, the reaction was started by adding nucleotides, LE19 RNA, and alpha-^{32}P-CTP. Aliquots were stopped at 15 min and 30 min and resolved in denaturing polyacrylamide gels. *De novo* (DN), primer extension (PE), and template switching (TS) products were quantified. Values are the averages and corresponding standard errors of the means (SEM) from at least four independent experiments. *, $P \leq 0.05$; **, $P \leq 0.01$. (B) Representative gel image of the values given in panel A. The positions of DN, PE, and TS products are indicated. Preincubation conditions as well as the times at which the RNA synthesis reaction was stopped are indicated below the image. (C) *In vitro* phosphorylation of NS5B by recombinant Akt under the reaction conditions used for panels A and B. NS5B-FP was used instead of NS5B to differentiate between HCV polymerase and Akt, as in Fig. 1. Buffer conditions were the same as those used for RNA synthesis. Positions of protein markers are indicated on the left.

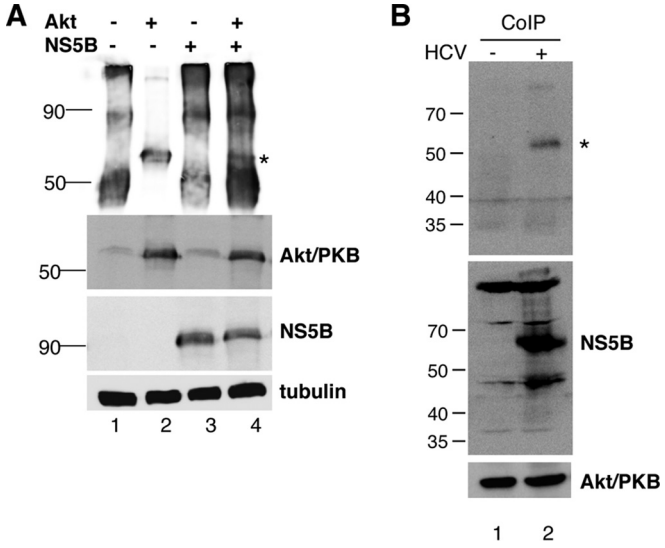

FIG 4 Coimmunoprecipitation of Akt/PKB and NS5B. (A) SDS-PAGE (10%) analysis of immunoprecipitated protein from lysates of Huh7.5 cells transiently transfected with pcDNA3 empty vector (control, lane 1), HA-tagged Akt/PKB (pcFEL, lane 2), NS5B-FP (pcDNA-Dest40-NS5B-FP, lane 3), and Akt/PKB plus NS5B-FP (lane 4). Cell protein extracts were immunoprecipitated with anti-GFP (lanes 1, 3, and 4) or anti-HA (lane 2) antibodies and then immunoblotted using an anti-Akt antibody (upper panel). The asterisk indicates the product of immunoprecipitation. Total cell lysates (50 μg) used in the coimmunoprecipitation experiment were fractionated on SDS-PAGE and immunostained using anti-Akt, anti-NS5B, and antitubulin antibodies (Akt/PKB, NS5B, and tubulin panels). (B) Coimmunoprecipitation experiment performed using extracts from HCVp0-infected Huh7.5 cells. Cell extracts were immunoprecipitated with an anti-NS5B antibody and then immunoblotted using an anti-Akt antibody (upper panel). The asterisk indicates the product of immunoprecipitation. Total cell lysates (50 μg) used in the coimmunoprecipitation experiment were fractionated and immunoblotted with anti-NS5B and anti-Akt antibodies (NS5B and Akt/PKB panels). Results show representative blots from three independent experiments with nearly identical results. Sizes of molecular markers are indicated on the left in kilodaltons.

The specificity of the qRT-PCRs was monitored by determining the denaturation curves of the amplified DNAs. Negative controls (without template RNA and/or with RNA from mock-infected cells) were run in parallel with each amplification reaction to ascertain the absence of contamination with undesired templates.

Immunofluorescence assays. The immunocytochemistry protocol was the same for transfected and HCVp0-infected Huh7.5 cells. Briefly, at the desired time points, cells situated on coverslips that were previously treated with poly-L-lysine (Sigma) were fixed in 4% paraformaldehyde for 10 min, permeabilized with 0.2% Triton X-100 for 10 min, washed in phosphate-buffered saline (PBS), and blocked with 5% bovine serum albumin (BSA; Sigma). Samples were incubated overnight in 0.5% BSA with primary antibodies (1:1,000) in various combinations, as indicated in the corresponding figures. After washing with PBS, samples were incubated with fluorescent secondary antibodies. Nuclei were visualized with 4′,6-diamidino-2-phenylindole (DAPI; Invitrogen). Images of the samples were taken using a Zeiss LSM-710 confocal microscope.

Statistical analyses. Statistical comparisons among groups were performed with Student's *t* tests. Significant differences ($P \leq 0.05$) between data sets are indicated. Those with *P* values of ≤0.01 were considered highly significant.

RESULTS

***In vitro* phosphorylation of NS5B by Akt/PKB.** Akt/PKB phosphorylates Ser and Thr residues within the minimal consensus sequence ArgXArgXX(Ser/Thr)h, where X is any amino acid and h is a bulky hydrophobic amino acid (22, 26). We scanned the HCV polyprotein amino acid sequence using Scansite software (27) and observed an accumulation of exposed putative Akt-driven phosphorylation sites in NS5B (Fig. 1A and B). Relative residue surface accessibility was investigated using the NetSirfP program (28) and the "accessible surface area and accessibility calculation for protein" tool (Center for Informational Biology, Ochanomizu University; http://cib.cf.ocha.ac.jp/bitool/ASA/). Nine NS5B residues were recognized as possible targets of Akt/PKB (Fig. 1A). Amino

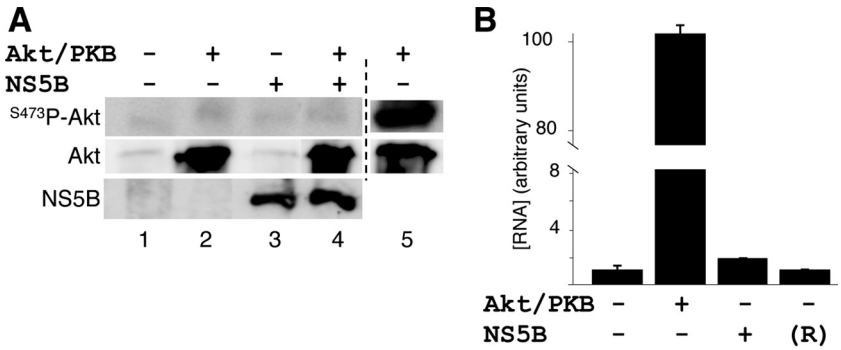

FIG 5 Effects of NS5B on Akt/PKB mRNA and protein levels. (A) Akt/PKB protein detection. Huh7.5 cells expressing Akt/PKB and/or NS5B were collected and lysed, and 50 μg of total cell lysates was fractionated and blotted against Ser473-phosphorylated Akt/PKB (upper part), Akt/PKB (middle part), or NS5B (lower part). Lane 5 was loaded with activated Akt/PKB (from insulin-treated cells) as a positive control of ^{S473}P-Akt antibody. (B) Akt/PKB mRNA quantification. Real-time RT-PCR results obtained with Huh7.5 cells transiently transfected with Akt/PKB, NS5B, or Huh7.5 cells carrying the pI389/NS3-3′/LucUbiNeo-ET HCV subgenomic replicon (R). Measurements from cells without Akt/PKB transfection correspond to endogenous Akt/PKB mRNA. Average values and standard deviations for two independent experiments performed in triplicate are shown. Procedures are described in Materials and Methods.

acids Thr227 and Thr389 were buried, with low relative surface accessibilities of 9% and 10%, respectively, while residues Ser453, Thr53, Thr520, Ser84, Ser506, Ser46, and Ser513 displayed relative surface accessibilities ranging from 14% to 79% (Fig. 1A and B). Furthermore, the exposed residues are located in flexible subdomains that may alter their exposure during the catalytic cycle (29). Therefore, the majority of the putative Akt/PKB phosphorylation sites in NS5B are sufficiently surface exposed to be a substrate for this kinase.

When investigating HCV NS5B *in vitro* phosphorylation by Akt/PKB, it is important to distinguish between phosphorylation of NS5B and Akt/PKB self-phosphorylation because the two proteins have a similar molar mass of about 65 kDa (Fig. 1C). For this reason, an *in vitro* phosphorylation assay was performed using a recombinant NS5B fused to the GFP derivative citrine (NS5B-FP) that renders a fusion protein of 90 kDa (19). The assay revealed phosphorylation of both proteins, but phosphorylation of NS5B-FP was dependent on the presence of Akt/PKB (Fig. 1D). Akt/PKB inhibitor MK-2206 inhibited NS5B phosphorylation in a concentration-dependent manner (Fig. 1D). No phosphorylation of recombinant citrine (27 kDa) (Fig. 1C) by Akt/PKB was observed (Fig. 1E). We concluded that Akt/PKB phosphorylates HCV NS5B *in vitro*.

Ser or Thr residues at positions 53, 84, 227, and 543 were totally conserved among genotypes 1 to 7 (see Fig. S1A in the supplemental material). Thr at position 389 was almost totally conserved for genotypes 1, 2, 3, and 7, and Ser at position 506 was conserved only for genotype 1 (see Fig. S1A in the supplemental material). These six positions with different levels of conservation among genotypes were mutated to Ala in the context of the NS5B-FP fusion protein (see Fig. S1B in the supplemental material). We also constructed and purified the double mutant T53A/S506A, because both positions are involved in NS5B-NS5B interactions and modifications in their side chains might affect protein-protein contacts (29). The resulting proteins were overexpressed, and purified proteins were subjected to the *in vitro* kinase assay as described above. None of these mutants lost their ability to be phosphorylated by Akt (Fig. 1F). This result indicates that Akt phosphorylates more than one residue or that Akt phosphorylates NS5B in noncanonical or nonconserved sequences.

Effect of Akt/PKB inhibition on HCV replication. To confirm the implication of Akt/PKB in the replicative cycle of HCV, experiments were performed using our *in vivo* experimental system (23). Previous studies have established that some Akt/PKB inhibitors such as Akt-II and Akt-V, as well as siRNAs targeting Akt, impair HCV replication (13, 14). MK-2206 is a highly selective inhibitor of Akt currently in clinical trials (https://clinicaltrials.gov). MK-2206 has a 50% inhibitory concentration (IC_{50}) in the low nanomolar range, and it does not show inhibitory activities against 250 other protein kinases. For these reasons and because this inhibitor was not used in HCV propagation experiments before, MK-2206 was tested in HCVp0-infected Huh7.5 cells, as described in Materials and Methods. Viral RNA from MK-2206-treated and untreated cells was quantified at different postinfection time points (Fig. 2). Viral infectivity in the cell culture supernatant showed little variation at 7 h p.i. However, it decreased in an inhibitor dose-dependent manner at 48 h p.i. (Fig. 2A). Intracellular viral RNA slightly increased with elevated inhibitor concentrations at 7 h p.i., whereas it remained invariant at 48 h p.i. (Fig. 2B). We compared the values obtained at 48 h and 7 h as a measure of how the infection was being developed in both treated and untreated cells for each experimental condition. Both HCV infectivity and HCV RNA ratios showed statistically significant decreases in an inhibitor dose-dependent manner (Fig. 2C and D). Cellular viability was not significantly altered (Fig. 2E).

Effect of NS5B phosphorylation on polymerase activity. NS5B is phosphorylated by Akt (Fig. 1C and D), and Akt inhibition induced a decrease in HCV infectivity (Fig. 2). To analyze the effect of NS5B phosphorylation on RNA-dependent RNA polymerase activity, HCV NS5B was preincubated at room temperature with recombinant Akt or with Akt in combination with ATP as described in Materials and Methods. After this, the RNA synthesis reaction was started by adding nucleotides and radioisotope and stopped after 15 or 30 min (Fig. 3A and B). Akt is able to phosphorylate NS5B under these

conditions (Fig. 3C). The presence of Akt and especially Akt plus ATP inhibited the RNA polymerase activity of NS5B. This effect was strongest upon 30 min of reaction. All reactions carried out by HCV NS5B, that is, *de novo* initiation (DN), primer extension (PE), and template switching (TS), were affected (Fig. 3A and B). Therefore, the presence of Akt in the reaction mixture, and especially NS5B phosphorylation by Akt, decreased polymerase activity.

Interaction of Akt/PKB with NS5B. Next, we tested a possible *in vivo* interaction between NS5B and Akt/PKB. A lysate from cells transiently cotransfected with plasmids encoding Akt/PKB (tagged with an HA epitope in the plasmid pcFEL) and NS5B-FP (pcDNA-Dest40-NS5B-citrine) was immunoprecipitated with anti-GFP (to precipitate NS5B-FP) and blotted with anti-HA (to visualize Akt/PKB). A band of a molar mass compatible with Akt/PKB was obtained (Fig. 4A). To confirm this result, cell lysate was immunoprecipitated with anti-HA and blotted with anti-GFP. A band of a molar mass compatible with NS5B-FP was obtained (see Fig. S2 in the supplemental material). To examine the interaction in the context of the HCV polyprotein, coimmunoprecipitation experiments were additionally performed using HCV-infected Huh7.5 cells as described in Materials and Methods. In extracts of HCVp0-infected cells, a band with the expected size of the endogenous Akt/PKB was detected in the fraction immunoprecipitated with anti-NS5B (Fig. 4B). Therefore, NS5B also interacts with Akt/PKB in infected cells.

Next, we examined if the interaction of NS5B with Akt/PKB induced changes in cellular Akt/PKB at the level of mRNA or protein and also in the phosphorylation status of Akt/PKB. Transfection of Huh7.5 cells with a plasmid encoding NS5B-FP (pcDNA-Dest40-NS5B-citrine) did not change Akt/PKB protein levels, Akt/PKB activation, or Akt/PKB mRNA levels (Fig. 5). Thus, NS5B interacts with Akt/PKB without affecting Akt/PKB mRNA or protein.

Intracellular localization of Akt/PKB and NS5B. To identify the intracellular site of the interaction between Akt/PKB and HCV NS5B, Huh7.5 cells were transfected with plasmids encoding Akt/PKB (pcFEL) and NS5B-FP (pcDNA-Dest40-NS5B-citrine), and the expressed proteins were localized by confocal microscopy. In resting, unstimulated Huh7.5 cells, Akt/PKB was uniformly distributed in the cytoplasm, as previously described (30), and the NS5B distribution was perinuclear, also as expected from previous results (31) (Fig. 6A, Akt-HA and NS5B-FP panels). In contrast, in Huh7.5 cells cotransfected with plasmids expressing the two proteins, the subcellular localization of Akt/PKB changed dramatically, and it colocalized with NS5B in the perinuclear region (Fig. 6A). The subcellular Akt/PKB distribution depended on the expression of HCV NS5B (compare solid and dashed arrows), and the perinuclear location was observed in 95% of the analyzed cells ($n = 150$) (Fig. 6B). The same perinuclear colocation of Akt/PKB and HCV NS5B occurred in Huh7.5 cells stably expressing HCV nonstructural proteins from the pI389/NS3-3′/LucUbiNeo-ET subgenomic replicon (Fig. 7), with perinuclear colocalization in 87% of the analyzed cells ($n = 150$) (Fig. 7B).

To exclude that perinuclear colocalization could be a mere side effect of overexpression of the relevant proteins, immunocytochemistry was performed with Huh7.5 cells either uninfected or infected with HCVp0 (Fig. 8). Uninfected cells showed Akt/PKB homogeneously distributed in the cytoplasm and the absence of NS5B, as expected (Fig. 8A, Akt-C and NS5B-C panels). However, in HCVp0-infected cells Akt/PKB and HCV NS5B colocalized in the perinuclear region (Fig. 8A). Akt/PKB relocalization from the cytoplasm to the perinuclear region was related to expression of NS5B (Fig. 8A, compare solid and dashed arrows). The perinuclear colocalization was observed in 82% of the analyzed cells ($n = 150$) (Fig. 8B). Therefore, the NS5B-Akt/PKB interaction resulted in the subcellular relocalization of Akt/PKB from cytoplasmic to perinuclear regions, independently of the system used for the intracellular expression of these proteins.

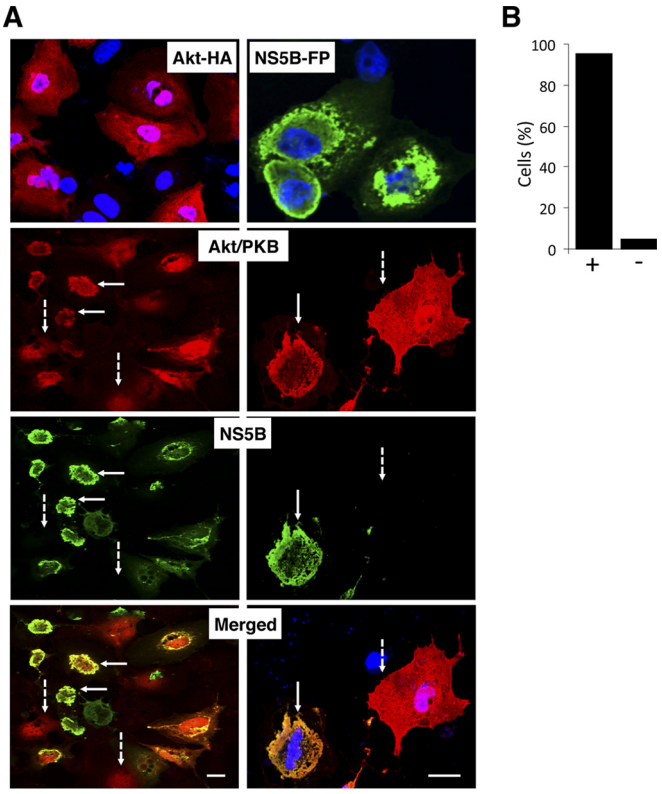

FIG 6 Intracellular localization of NS5B-FP and Akt/PKB. (A) Huh7.5 cells transiently transfected with plasmids encoding Akt/PKB (pcFEL) and/or NS5B-FP (pcDNA-Dest40-NS5B-citrine). Immunocytochemistry was performed using antibodies against HA (in red), detecting Akt/PKB, or against GFP (in green), detecting NS5B-FP and with DAPI (in blue), detecting cell nuclei. Upper panels are micrographs showing cells transfected with a single plasmid encoding either Akt/PKB (left) or NS5B-FP (right). Nuclear staining in these panels was performed with DAPI. Panels named Akt/PKB, NS5B, and Merged correspond to transfection experiments with both Akt/PKB and NS5B-FP. Left panels correspond to a confocal microscopy field in which cells transfected with only Akt/PKB (dashed arrow) and cells transfected with both Akt/PKB and NS5B (solid arrow) are shown. Panels on the right show only two representative cells, one transiently cotransfected with both plasmids (solid arrow) and one transiently transfected with only a plasmid encoding Akt/PKB (dashed arrow). Akt panels correspond to immunostaining with anti-HA, whereas NS5B panels correspond to anti-GFP staining. Merged images (bottom panels) show an overlay with colocalization in orange. Scale bars, 10 μm. (B) Percentage of cells in which Akt-NS5B colocalization was observed. Procedures are described in Materials and Methods.

DISCUSSION

The results reported here show interaction between the cellular kinase Akt/PKB and NS5B, resulting in colocalization of the

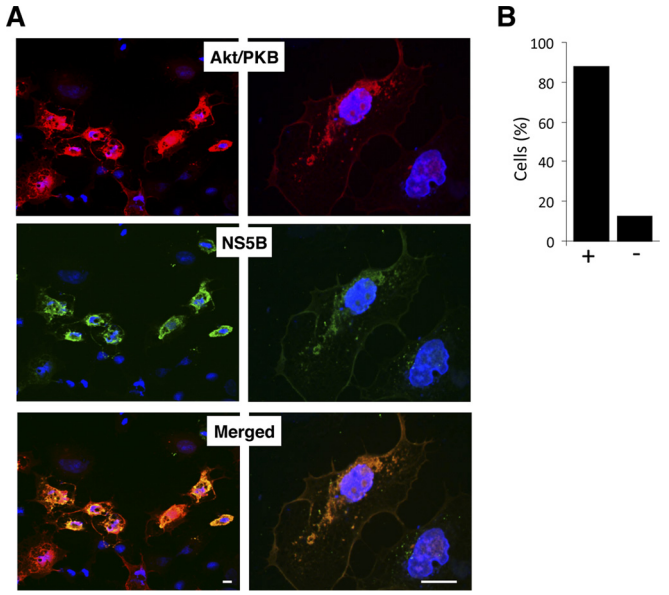

FIG 7 Subcellular localization of Akt/PKB and NS5B expressed from an HCV replicon. (A) Immunocytochemistry of Huh7.5 cells carrying HCV subgenomic replicon pI389/NS3-3′/LucUbiNeo-ET using antibodies against endogenous Akt/PKB (in red, upper panels), against HCV NS5B (in green, middle panels), and with DAPI (in blue), detecting cell nuclei. The overlay shows colocalization in orange. Left panels correspond to a confocal microscopy field, whereas the panels on the right show only two representative cells. Scale bars,10 μm. (B) Percentage of cells where Akt-NS5B colocalization was observed. Procedures are described in Materials and Methods.

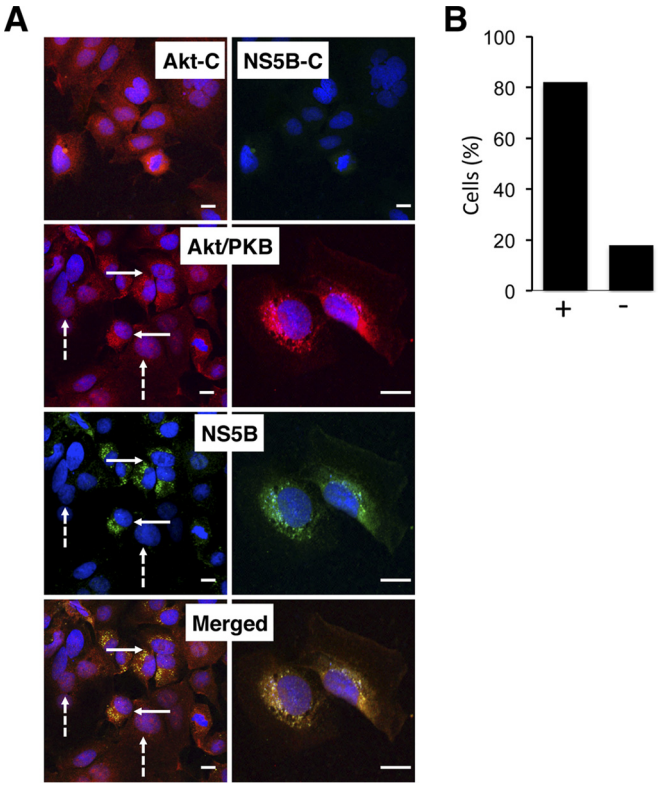

FIG 8 Intracellular localization of Akt/PKB and NS5B expressed from HCVp0. (A) Immunocytochemistry of Huh7.5 cells infected with HCVp0 and visualized with antibodies against Akt/PKB (in red) or NS5B (green) and with DAPI. Top panels are uninfected control cells visualized with anti-Akt (left) and anti-NS5B (right) antibodies. Akt/PKB, NS5B, and merged panels correspond to HCVp0-infected cells. In the merged images (bottom panel), colocalization is shown in orange. Left panels correspond to a confocal microscopy field, whereas right panels show a magnification with representative cells. Solid-line arrows show cells where Akt/PKB colocalizes with NS5B, whereas dashed-line arrows point at uninfected cells. The images show a field representative of at least three independent experiments. Scale bars, 10 μm. (B) Percentage of cells in which Akt-NS5B colocalization was observed. Methodological details are described in Materials and Methods.

two proteins in the perinuclear region of the infected cell. This places Akt/PKB among other host factors that are relevant for the HCV infection cycle in terms of their interaction with HCV NS5B, for example, the cellular proteins human vesicle-associated membrane-associated protein of 33 kDa (hVAP-33), PRK2, estrogen receptor, and the retinoblastoma tumor suppressor protein (pRb), among others (32–34). Interventions targeting virus-host interactions could be relevant for antiviral drug development.

It has been previously shown that HCV infection inhibits the PI3K/Akt/mTOR pathway and that inhibition of Akt/PKB results in a reduction of HCV replication and a large decrease in the number of HCV-infected cells (13, 14). Our results with the Akt/PKB inhibitor MK-2206 are consistent with these previous observations and show a delay of the infection and a decrease in the amount of progeny virus (Fig. 2C and D). Probably due to differences in the MOI at which the experiments were performed (0.5 in this study, 10 in other studies), the effect was not as pronounced as in previous studies; nevertheless, the inhibition pointed at a possible participation of NS5B in the effect of Akt/PKB. We have also shown that Akt/PKB can phosphorylate *in vitro* the HCV NS5B protein. *In vitro* kinase assay results obtained with NS5B carrying point mutations at positions susceptible to be phosphorylated by Akt/PKB have not been conclusive to map phosphorylation sites. However, incubation of NS5B with Akt alone or with Akt plus ATP to carry out NS5B phosphorylation resulted in a pronounced decrease of RNA polymerase activity (Fig. 3). Attenuation of RNA synthesis was strongest when phosphorylation took place, but to a lesser extent, it also occurred in the presence of solely Akt (Fig. 3). This result is consistent with the increase in the amount of intracellular HCV RNA detected in cells treated with an Akt inhibitor at a short time after infection (7 h p.i.) (Fig. 2). RNA synthesis defects in HCV NS5B mutants that mimic phosphorylation at Ser residues have been previously reported (35). In any case, further experiments with proteins carrying different combinations of mutated residues as well as with deletion mutants should be performed to precisely map the residues that are phosphorylated by Akt/PKB and its subsequent effects on polymerase activity and subcellular localization.

Changes in subcellular protein localization are relevant for regulatory processes. Actually, Akt/PKB can form complexes with other proteins that do not have to be substrates for its kinase activity but rather can act as modulators of Akt/PKB biological activity and function (36, 37). Our results show for the first time that HCV NS5B interacts with Akt/PKB (Fig. 4; see also Fig. S2 in the supplemental material). Moreover, Akt/PKB is relocated to the perinuclear region of infected cells, where it colocalizes with

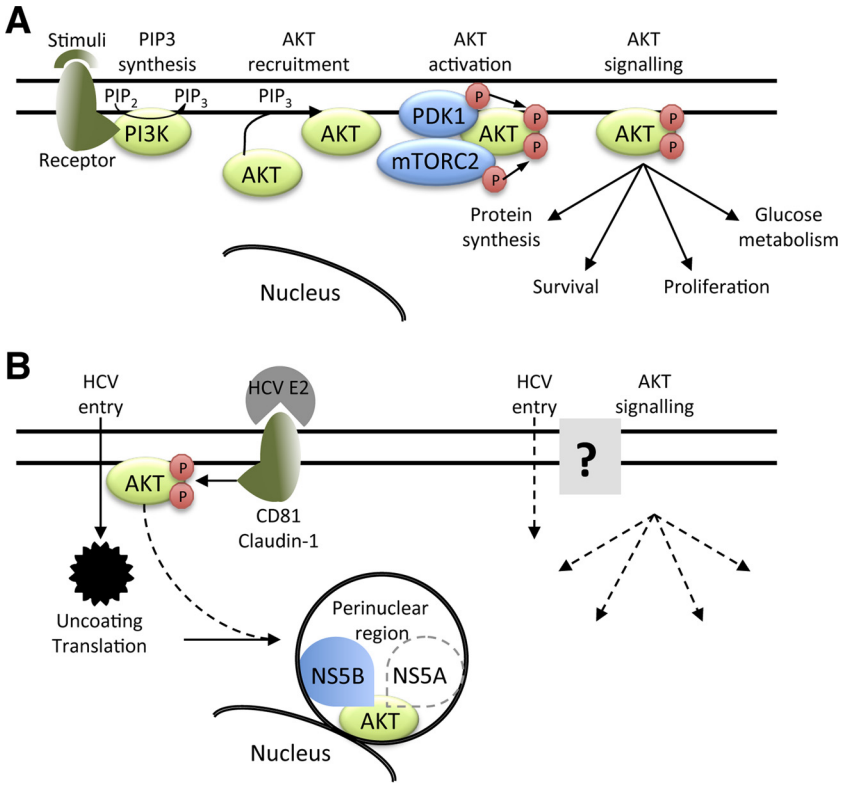

FIG 9 (A) Model of Akt activation. Upon interaction of some cellular receptors with specific ligands, the phosphatidylinositol 4,5 bisphosphate 3 kinase (PI3K) synthesizes phosphatidylinositol 3-phosphate (PIP_3), which in turn binds Akt/PKB to relocate it to the plasma membrane. At this location, Akt/PKB is phosphorylated by phosphoinositide-dependent kinase 1 (PDK1) and the mammalian target of rapamycin complex 2 (mTORC2) to become activated. Activated Akt/PKB can activate or deactivate its myriad substrates with effects on protein synthesis, cell survival and proliferation, and glucose metabolism among others (4). (B) Effects of HCV infection on Akt/PKB. Upon interaction of the HCV E2 surface glycoprotein with specific receptors (including CD81 and Claudin-1), Akt/PKB is activated, promoting HCV entry into the cell. Once HCV uncoats and translates its positive RNA genome, viral proteins are produced, including the viral polymerase (NS5B). HCV NS5B interacts with Akt/PKB, inducing its subcellular relocalization to the perinuclear region (this study), where interactions with other HCV proteins (such as NS5A) can occur. This relocalization might affect entry of new HCV particles into the cell (superinfection exclusion) as well as Akt/PKB signaling.

NS5B (Fig. 6 to 8), suggesting a possible function of Akt/PKB in the replication complex (15, 38–40). HCV NS5A is a component of the HCV replication complexes and is phosphorylated and hyperphosphorylated by cellular kinases, including Akt/PKB (12) and casein kinase Iα (41). Analogous to our observations, there is evidence that simian virus 40 (SV40) T antigen may contribute to a change in the subcellular localization of Akt/PKB from the nucleus to the cytoplasm, as judged from a comparison of the intracellular location of Akt/PKB in transformed and nontransformed HEK-293 cells (42).

Akt/PKB activation in Huh7.5 cells occurs at the cytosolic face of the plasma membrane where activators (PI3P) and kinases (PDK1 and mTORC2) are located (Fig. 9A). Transient, E2 glycoprotein-mediated Akt/PKB activation has been previously related to HCV entry into the cell (13). Related to viral entry, some authors have described a superinfection exclusion mechanism by which cells currently infected with HCV are resistant to a secondary infection with the same or a closely related virus (43–45). These authors suggest that the first virus prevents secondary infections because it sequesters a limiting host factor (44, 45). Our results suggest that HCV NS5B might be the HCV protein that mediates Akt/PKB relocalization to fulfill a function in the replication complexes. Relocalization of Akt/PKB by HCV NS5B might also prevent further Akt/PKB activation in the plasma membrane governed by the E2 glycoprotein from new virions. In any case, further experiments are needed to resolve the possible role played by Akt/PKB and HCV NS5B in the superinfection exclusion process seen for HCV as well as to map the NS5B and Akt/PKB contact surface.

Based on our results, we propose a model (Fig. 9B) in which the E2 glycoprotein activates Akt/PKB, allowing HCV entry (13, 14) and, following virus uncoating and translation, viral polymerase NS5B sequesters and relocates Akt/PKB to the perinuclear region, where it can interact with other HCV proteins (12). Furthermore, this interaction could deplete Akt/PKB from the plasma membrane, consequently diminishing its subsequent activation and preventing superinfection. Identification of the cellular and viral components (both protein and RNA) that form part of the perinuclear region where Akt/PKB and NS5B colocalize is currently in progress in our laboratory. Although many aspects of this model require experimental verification, the current picture is that cellular pathways involved in cell cycle, apoptosis, autophagy, and metabolism must be finely regulated by viral components to the virus's benefit. Interaction with and, most importantly, relocalization of cellular Akt/PKB could be the way for HCV to control the PI3K/Akt/

mTOR pathway during the HCV life cycle (Fig. 8B). A deeper knowledge of the NS5B-Akt/PKB molecular interaction could be used to design small-molecule inhibitors directed to interfere with this critical connection, by analogy to the proposed new Bcl-2 inhibitors for cancer treatment (46). Furthermore, Akt/PKB inhibitors currently undergoing clinical trials could be useful for HCV infection treatment, as it has been recently showed for those inhibiting mTORC1 (17). Taken together, these results highlight the importance of the PI3K/Akt/mTOR pathway in HCV infection.

ACKNOWLEDGMENTS

The Huh7.5 cell line and plasmid pI389/NS3-3′/LucUbiNeo-ET were kindly supplied by R. Bartenschlager (University of Heidelberg). Sandra Franco is acknowledged for her help with replicon experiments. Piet de Groot is acknowledged for critical reading of the manuscript.

FUNDING INFORMATION

This work was supported by grants of the European Research Council (ERC-2011-StG-281191-VIRMUT to Antonio Mas), the Ministerio de Ciencia e Innovación (BFU2010-18767 to Antonio Mas, BFU2011-23604 to Esteban Domingo, and SAF2012-30862 and SAF2015-62215-R to Ricardo Sánchez-Prieto), and the Consejería de Educación de Castilla-La Mancha (PPII10-0243-6857 to Antonio Mas, and PPII10-0141-0404 to Ricardo Sánchez-Prieto). Fundación Leticia Castillejo is also acknowledged. Work at CBMSO was supported also by Fundación Ramón Areces. CIBERehd is funded by Instituto de Salud Carlos III. Celia Perales is supported by the Miguel Servet program (Instituto de Salud Carlos III). The funders had no role in study design, data collection and interpretation, or the decision to submit the work for publication.

REFERENCES

1. **Toshikuni N, Arisawa T, Tsutsumi M.** 2014. Hepatitis C-related liver cirrhosis—strategies for the prevention of hepatic decompensation, hepatocarcinogenesis, and mortality. World J Gastroenterol **20:**2876–2887. http://dx.doi.org/10.3748/wjg.v20.i11.2876.
2. **Bode JG, Brenndorfer ED, Karthe J, Haussinger D.** 2009. Interplay between host cell and hepatitis C virus in regulating viral replication. Biol Chem **390:**1013–1032. http://dx.doi.org/10.1515/BC.2009.118.
3. **Song G, Ouyang G, Bao S.** 2005. The activation of Akt/PKB signaling pathway and cell survival. J Cell Mol Med **9:**59–71. http://dx.doi.org/10.1111/j.1582-4934.2005.tb00337.x.
4. **Vivanco I, Sawyers CL.** 2002. The phosphatidylinositol 3-kinase AKT pathway in human cancer. Nat Rev Cancer **2:**489–501. http://dx.doi.org/10.1038/nrc839.
5. **Hay N.** 2005. The Akt-mTOR tango and its relevance to cancer. Cancer Cell **8:**179–183. http://dx.doi.org/10.1016/j.ccr.2005.08.008.
6. **Heras-Sandoval D, Perez-Rojas JM, Hernandez-Damian J, Pedraza-Chaverri J.** 2014. The role of PI3K/AKT/mTOR pathway in the modulation of autophagy and the clearance of protein aggregates in neurodegeneration. Cell Signal **26:**2694–2701. http://dx.doi.org/10.1016/j.cellsig.2014.08.019.
7. **Gingras AC, Kennedy SG, O'Leary MA, Sonenberg N, Hay N.** 1998. 4E-BP1, a repressor of mRNA translation, is phosphorylated and inactivated by the Akt(PKB) signaling pathway. Genes Dev **12:**502–513. http://dx.doi.org/10.1101/gad.12.4.502.
8. **Lee CJ, Liao CL, Lin YL.** 2005. Flavivirus activates phosphatidylinositol 3-kinase signaling to block caspase-dependent apoptotic cell death at the early stage of virus infection. J Virol **79:**8388–8399. http://dx.doi.org/10.1128/JVI.79.13.8388-8399.2005.
9. **Ehrhardt C, Wolff T, Pleschka S, Planz O, Beermann W, Bode JG, Schmolke M, Ludwig S.** 2007. Influenza A virus NS1 protein activates the PI3K/Akt pathway to mediate antiapoptotic signaling responses. J Virol **81:**3058–3067. http://dx.doi.org/10.1128/JVI.02082-06.
10. **Ji WT, Liu HJ.** 2008. PI3K-Akt signaling and viral infection. Recent Pat Biotechnol **2:**218–226. http://dx.doi.org/10.2174/187220808786241042.
11. **Eden JS, Sharpe LJ, White PA, Brown AJ.** 2011. Norovirus RNA-dependent RNA polymerase is phosphorylated by an important survival kinase, Akt. J Virol **85:**10894–10898. http://dx.doi.org/10.1128/JVI.05562-11.
12. **Randall G, Panis M, Cooper JD, Tellinghuisen TL, Sukhodolets KE, Pfeffer S, Landthaler M, Landgraf P, Kan S, Lindenbach BD, Chien M, Weir DB, Russo JJ, Ju J, Brownstein MJ, Sheridan R, Sander C, Zavolan M, Tuschl T, Rice CM.** 2007. Cellular cofactors affecting hepatitis C virus infection and replication. Proc Natl Acad Sci U S A **104:**12884–12889. http://dx.doi.org/10.1073/pnas.0704894104.
13. **Liu Z, Tian Y, Machida K, Lai MM, Luo G, Foung SK, Ou JH.** 2012. Transient activation of the PI3K-AKT pathway by hepatitis C virus to enhance viral entry. J Biol Chem **287:**41922–41930. http://dx.doi.org/10.1074/jbc.M112.414789.
14. **Huang H, Kang R, Wang J, Luo G, Yang W, Zhao Z.** 2013. Hepatitis C virus inhibits AKT-tuberous sclerosis complex (TSC), the mechanistic target of rapamycin (MTOR) pathway, through endoplasmic reticulum stress to induce autophagy. Autophagy **9:**175–195. http://dx.doi.org/10.4161/auto.22791.
15. **Sir D, Kuo CF, Tian Y, Liu HM, Huang EJ, Jung JU, Machida K, Ou JH.** 2012. Replication of hepatitis C virus RNA on autophagosomal membranes. J Biol Chem **287:**18036–18043. http://dx.doi.org/10.1074/jbc.M111.320085.
16. **Chatel-Chaix L, Bartenschlager R.** 2014. Dengue virus- and hepatitis C virus-induced replication and assembly compartments: the enemy inside—caught in the web. J Virol **88:**5907–5911. http://dx.doi.org/10.1128/JVI.03404-13.
17. **Stohr S, Costa R, Sandmann L, Westhaus S, Pfaender S, Anggakusuma Dazert E, Meuleman P, Vondran FW, Manns MP, Steinmann E, von Hahn T, Ciesek S.** 2015. Host cell mTORC1 is required for HCV RNA replication. Gut http://dx.doi.org/10.1136/gutjnl-2014-308971.
18. **Viniegra JG, Martinez N, Modirassari P, Hernandez Losa J, Parada Cobo C, Sanchez-Arevalo Lobo VJ, Aceves Luquero CI, Alvarez-Vallina L, Ramon y Cajal S, Rojas JM, Sanchez-Prieto R.** 2005. Full activation of PKB/Akt in response to insulin or ionizing radiation is mediated through ATM. J Biol Chem **280:**4029–4036. http://dx.doi.org/10.1074/jbc.M410344200.
19. **Clemente-Casares P, Lopez-Jimenez AJ, Bellon-Echeverria I, Encinar JA, Martinez-Alfaro E, Perez-Flores R, Mas A.** 2011. De novo polymerase activity and oligomerization of hepatitis C virus RNA-dependent RNA-polymerases from genotypes 1 to 5. PLoS One **6:**e18515. http://dx.doi.org/10.1371/journal.pone.0018515.
20. **Frese M, Barth K, Kaul A, Lohmann V, Schwarzle V, Bartenschlager R.** 2003. Hepatitis C virus RNA replication is resistant to tumour necrosis factor-alpha. J Gen Virol **84:**1253–1259. http://dx.doi.org/10.1099/vir.0.18997-0.
21. **Bellon-Echeverria I, Lopez-Jimenez AJ, Clemente-Casares P, Mas A.** 2010. Monitoring hepatitis C virus (HCV) RNA-dependent RNA polymerase oligomerization by a FRET-based in vitro system. Antiviral Res **87:**57–66. http://dx.doi.org/10.1016/j.antiviral.2010.04.009.
22. **Alessi DR, Caudwell FB, Andjelkovic M, Hemmings BA, Cohen P.** 1996. Molecular basis for the substrate specificity of protein kinase B; comparison with MAPKAP kinase-1 and p70 S6 kinase. FEBS Lett **399:**333–338. http://dx.doi.org/10.1016/S0014-5793(96)01370-1.
23. **Perales C, Beach NM, Gallego I, Soria ME, Quer J, Esteban JI, Rice C, Domingo E, Sheldon J.** 2013. Response of hepatitis C virus to long-term passage in the presence of alpha interferon: multiple mutations and a common phenotype. J Virol **87:**7593–7607. http://dx.doi.org/10.1128/JVI.02824-12.
24. **Sheldon J, Beach NM, Moreno E, Gallego I, Pineiro D, Martinez-Salas E, Gregori J, Quer J, Esteban JI, Rice CM, Domingo E, Perales C.** 2014. Increased replicative fitness can lead to decreased drug sensitivity of hepatitis C virus. J Virol **88:**12098–12111. http://dx.doi.org/10.1128/JVI.01860-14.
25. **de la Cruz-Morcillo MA, Valero ML, Callejas-Valera JL, Arias-Gonzalez L, Melgar-Rojas P, Galan-Moya EM, Garcia-Gil E, Garcia-Cano J, Sanchez-Prieto R.** 2012. P38MAPK is a major determinant of the balance between apoptosis and autophagy triggered by 5-fluorouracil: implication in resistance. Oncogene **31:**1073–1085. http://dx.doi.org/10.1038/onc.2011.321.
26. **Obata T, Yaffe MB, Leparc GG, Piro ET, Maegawa H, Kashiwagi A, Kikkawa R, Cantley LC.** 2000. Peptide and protein library screening defines optimal substrate motifs for AKT/PKB. J Biol Chem **275:**36108–36115. http://dx.doi.org/10.1074/jbc.M005497200.
27. **Obenauer JC, Cantley LC, Yaffe MB.** 2003. Scansite 2.0: proteome-wide

prediction of cell signaling interactions using short sequence motifs. Nucleic Acids Res **31:**3635–3641. http://dx.doi.org/10.1093/nar/gkg584.
28. **Petersen B, Petersen TN, Andersen P, Nielsen M, Lundegaard C.** 2009. A generic method for assignment of reliability scores applied to solvent accessibility predictions. BMC Struct Biol **9:**51. http://dx.doi.org/10.1186/1472-6807-9-51.
29. **Lopez-Jimenez AJ, Clemente-Casares P, Sabariegos R, Llanos-Valero M, Bellon-Echeverria I, Encinar JA, Kaushik-Basu N, Froeyen M, Mas A.** 2014. Hepatitis C virus polymerase-polymerase contact interface: significance for virus replication and antiviral design. Antiviral Res **108:**14–24. http://dx.doi.org/10.1016/j.antiviral.2014.04.009.
30. **Meili R, Ellsworth C, Lee S, Reddy TB, Ma H, Firtel RA.** 1999. Chemoattractant-mediated transient activation and membrane localization of Akt/PKB is required for efficient chemotaxis to cAMP in Dictyostelium. EMBO J **18:**2092–2105. http://dx.doi.org/10.1093/emboj/18.8.2092.
31. **Hwang SB, Park KJ, Kim YS, Sung YC, Lai MM.** 1997. Hepatitis C virus NS5B protein is a membrane-associated phosphoprotein with a predominantly perinuclear localization. Virology **227:**439–446. http://dx.doi.org/10.1006/viro.1996.8357.
32. **Hundt J, Li Z, Liu Q.** 2013. Post-translational modifications of hepatitis C viral proteins and their biological significance. World J Gastroenterol **19:**8929–8939. http://dx.doi.org/10.3748/wjg.v19.i47.8929.
33. **Hillung J, Ruiz-Lopez E, Bellon-Echeverria I, Clemente-Casares P, Mas A.** 2012. Characterization of the interaction between hepatitis C virus NS5B and the human oestrogen receptor alpha. J Gen Virol **93:**780–785. http://dx.doi.org/10.1099/vir.0.039396-0.
34. **Kim SJ, Kim JH, Kim YG, Lim HS, Oh JW.** 2004. Protein kinase C-related kinase 2 regulates hepatitis C virus RNA polymerase function by phosphorylation. J Biol Chem **279:**50031–50041. http://dx.doi.org/10.1074/jbc.M408617200.
35. **Han SH, Kim SJ, Kim EJ, Kim TE, Moon JS, Kim GW, Lee SH, Cho K, Yoo JS, Son WS, Rhee JK, Han SH, Oh JW.** 2014. Phosphorylation of hepatitis C virus RNA polymerases ser29 and ser42 by protein kinase C-related kinase 2 regulates viral RNA replication. J Virol **88:**11240–11252. http://dx.doi.org/10.1128/JVI.01826-14.
36. **Ferrigno P, Silver PA.** 1999. Regulated nuclear localization of stress-responsive factors: how the nuclear trafficking of protein kinases and transcription factors contributes to cell survival. Oncogene **18:**6129–6134. http://dx.doi.org/10.1038/sj.onc.1203132.
37. **Brazil DP, Park J, Hemmings BA.** 2002. PKB binding proteins. Getting in on the Akt. Cell **111:**293–303.
38. **Gao L, Aizaki H, He JW, Lai MM.** 2004. Interactions between viral nonstructural proteins and host protein hVAP-33 mediate the formation of hepatitis C virus RNA replication complex on lipid raft. J Virol **78:**3480–3488. http://dx.doi.org/10.1128/JVI.78.7.3480-3488.2004.
39. **McGivern DR, Villanueva RA, Chinnaswamy S, Kao CC, Lemon SM.** 2009. Impaired replication of hepatitis C virus containing mutations in a conserved NS5B retinoblastoma protein-binding motif. J Virol **83:**7422–7433. http://dx.doi.org/10.1128/JVI.00262-09.
40. **Gu M, Rice CM.** 2013. Structures of hepatitis C virus nonstructural proteins required for replicase assembly and function. Curr Opin Virol **3:**129–136. http://dx.doi.org/10.1016/j.coviro.2013.03.013.
41. **Masaki T, Matsunaga S, Takahashi H, Nakashima K, Kimura Y, Ito M, Matsuda M, Murayama A, Kato T, Hirano H, Endo Y, Lemon SM, Wakita T, Sawasaki T, Suzuki T.** 2014. Involvement of hepatitis C virus NS5A hyperphosphorylation mediated by casein kinase I-alpha in infectious virus production. J Virol **88:**7541–7555. http://dx.doi.org/10.1128/JVI.03170-13.
42. **Santi SA, Lee H.** 2010. The Akt isoforms are present at distinct subcellular locations. Am J Physiol Cell Physiol **298:**C580–591. http://dx.doi.org/10.1152/ajpcell.00375.2009.
43. **Schaller T, Appel N, Koutsoudakis G, Kallis S, Lohmann V, Pietschmann T, Bartenschlager R.** 2007. Analysis of hepatitis C virus superinfection exclusion by using novel fluorochrome gene-tagged viral genomes. J Virol **81:**4591–4603. http://dx.doi.org/10.1128/JVI.02144-06.
44. **Tscherne DM, Evans MJ, von Hahn T, Jones CT, Stamataki Z, McKeating JA, Lindenbach BD, Rice CM.** 2007. Superinfection exclusion in cells infected with hepatitis C virus. J Virol **81:**3693–3703. http://dx.doi.org/10.1128/JVI.01748-06.
45. **Webster B, Ott M, Greene WC.** 2013. Evasion of superinfection exclusion and elimination of primary viral RNA by an adapted strain of hepatitis C virus. J Virol **87:**13354–13369. http://dx.doi.org/10.1128/JVI.02465-13.
46. **Oltersdorf T, Elmore SW, Shoemaker AR, Armstrong RC, Augeri DJ, Belli BA, Bruncko M, Deckwerth TL, Dinges J, Hajduk PJ, Joseph MK, Kitada S, Korsmeyer SJ, Kunzer AR, Letai A, Li C, Mitten MJ, Nettesheim DG, Ng S, Nimmer PM, O'Connor JM, Oleksijew A, Petros AM, Reed JC, Shen W, Tahir SK, Thompson CB, Tomaselli KJ, Wang B, Wendt MD, Zhang H, Fesik SW, Rosenberg SH.** 2005. An inhibitor of Bcl-2 family proteins induces regression of solid tumours. Nature **435:**677–681. http://dx.doi.org/10.1038/nature03579.
47. **O'Farrell D, Trowbridge R, Rowlands D, Jager J.** 2003. Substrate complexes of hepatitis C virus RNA polymerase (HC-J4): structural evidence for nucleotide import and de-novo initiation. J Mol Biol **326:**1025–1035. http://dx.doi.org/10.1016/S0022-2836(02)01439-0.